Chemical Engineering Journal 276 (2015) 59–64

Contents lists available at ScienceDirect

Chemical Engineering Journal

journal homepage: www.elsevier.com/locate/cej

Bioreduction of nitrate in a hydrogen-based membrane biofilm reactor using CO_2 for pH control and as carbon source

Siqing Xia [a,*], Chenhui Wang [a], Xiaoyin Xu [a], Youneng Tang [b], Zuowei Wang [a], Zaoli Gu [a], Yun Zhou [a]

[a] State Key Laboratory of Pollution Control and Resource Reuse, College of Environmental Science and Engineering, Tongji University, Shanghai 200092, China
[b] Department of Civil and Environmental Engineering, Florida Agricultural & Mechanical University-Florida State University College of Engineering, Tallahassee, FL 32310, USA

HIGHLIGHTS

- MBfR with double bundles of hollow fibers (one for H_2 and the other for CO_2).
- The CO_2 diffusion coefficient in PVC membrane was 3.8375×10^{-7} m^2/d @ 25 °C.
- CO_2 for pH control and as carbon source.

GRAPHICAL ABSTRACT

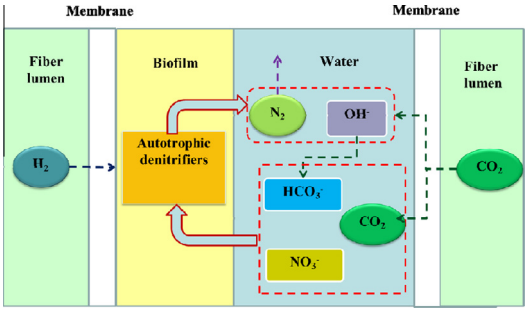

ARTICLE INFO

Article history:
Received 31 January 2015
Received in revised form 8 April 2015
Accepted 11 April 2015
Available online 18 April 2015

Keywords:
Nitrate
Hydrogen-based membrane biofilm reactor
CO_2
pH control
Carbon source

ABSTRACT

The hydrogen-based membrane biofilm reactor (MBfR) is efficient in removing nitrate in oligotrophic water, but pH increase due to denitrification is a tough problem in practice. To control pH, we investigated a novel MBfR with double bundles of hollow fibers (one for H_2 supply and the other for CO_2 supply). CO_2 was used for pH control and as the carbon source. The Fick's first law and steady state permeation tests were adopted to determine the CO_2 permeability of polyvinyl chloride (PVC) hollow fibers used in this study. The CO_2 diffusion coefficient in the membrane was 3.8375×10^{-7} m^2/d @ 25 °C. The CO_2 diffusion coefficient was verified by a nitrate bioreduction experiment in the MBfR. The calculated supply of CO_2 based on the CO_2 diffusion coefficient is consistent with the experimental results: The total nitrogen removal rate was more than 99% and the pH is stable at around 7.45. CO_2 diffused through the membrane is sufficient to be the sole carbon source. We confirmed that the novel MBfR with double bundles was stable and efficient. This research provides direct guidance to the design and operation of this new type MBfR.

1. Introduction

As a major technological breakthrough, the hydrogen-based membrane biofilm reactor (MBfR) combines the membrane and biofilm together creatively, which is a new choice to remove the oxidized contaminants in oligotrophic water such as groundwater and micro-polluted raw water without residual economically [1–3]. In the MBfR, hydrogen gas is delivered through the membrane in a bubbleless way and H_2 utilization efficiency can be more than 99% to avoid air explosive hazard, which make it come true that nontoxic and inexpensive H_2 compared to organic donors, can be the electron donor and energy source of the microorganism [3]. In recent years, the MBfR was investigated to remove several kinds of the oxidized contaminants in the oligotrophic water and gained high efficiency. Xia et al. [4] carried out a series of

* Corresponding author. Tel.: +86 21 65980440; fax: +86 21 65986313.
E-mail address: siqingxia@tongji.edu.cn (S. Xia).

http://dx.doi.org/10.1016/j.cej.2015.04.061
1385-8947/

Nomenclature

A_l, A_m	average surface area of the liquid and membrane film (m^2)
C_0, C_l	CO_2 concentrations in the lumen of the fibers and bulk liquid of the reactor (g CO_2/m^3)
C_i, C_e	CO_2 concentrations in the influent and effluent of the reactor (g CO_2/m^3)
$C_{NO_3^-}$	NO_3^- concentrations in the influent of the reactor (g/m^3)
C_{O_2}	O_2 concentrations in the influent of the reactor (g/m^3)
d_m	hollow fiber outer diameter (m)
d_l	liquid film outer diameter (m)
D_l	CO_2 diffusion coefficient in water @ 25 °C 1.74528×10^{-4} (m^2/d) [34]
D_m	CO_2 diffusion coefficient in the membrane (m^2/d)
h	water depth in the reactor (m)
H	Henry's Law constant of CO_2 3115.22 (m^3 Pa/mol) [35]
J_l	CO_2 flux through the liquid film (g $CO_2/(m^2\ d)$)
J_m	CO_2 flux through the membrane (g $CO_2/(m^2\ d)$)
L_{m1}	H_2 hollow fiber length (m)
L_{m2}	CO_2 hollow fiber length (m)
M	molar mass 44 (g/mol)
n_m	number of hollow fibers
P_0	CO_2 pressure in the hollow-fiber lumen (Mpa)
Q	water flow rate of the influent (m^3/d)
Q_t	total water flow rate in the reactor (m^3/d)
Q_1	wastewater flow rate in the reactor (m^3/d)
S	valid cross-section (m^2)
u	representative flow shear velocity in the reactor (m/d)
V	valid reactor volume (m^3)
z_l	liquid film thickness (m)
z_m	membrane thickness (m)

short-term experiments, which showed that nitrate reduction rate improved with H_2 pressure increasing, and over 97% of total nitrogen removal rate was achieved when the nitrate loading increased from 0.17 to 0.34 g NO_3^-–N/(m^2 day) without nitrite accumulation. Nerenberg et al. [5] conducted short-term tests without allowing time for the reactor to adapt to the contaminants and the result showed nitrate and oxygen were reduced by over 99% for all tests and removal for the contaminants ranged from a minimum of 29% for chlorate to over 95% for bromate.

Nitrate is a common oxidized contaminant in the groundwater. It is introduced into groundwater from a variety of sources such as agricultural activities, poor sewer systems, wastewater, and industrial activities [6]. Contamination of water by nitrate is increasing worldwide and nitrate level in natural waters becomes an important indicator of water quality. It is also a primary drinking water contaminant and standards have been set to regulate the maximum concentration level (MCL) of nitrate in potable water at 10 mg NO_3^--N/L in the US and China. Besides, as nitrogen source of microorganisms, nitrate is a key factor in the process of oxidized contaminants bioreduction. However one important characteristic of denitrification is that it produces approximately one equivalent of strong base for each equivalent of N reduced to nitrogen [7]. The pH will increase with the reaction going on if no measure is taken, while the optimal pH range reported for denitrification is 7–9 [8]. Once the pH value is beyond this range, it will inhibit the denitrification process and lead to accumulation of intermediates such as NO_2^- and N_2O [9–11]. The second consequence is precipitation of hardness cations that are common in the groundwater. Common mineral precipitates in biological denitrification processes includes calcium carbonate ($CaCO_3$), calcium hydrogen phosphate ($CaHPO_4$), calcium dihydrogen phosphate ($Ca(H_2PO_4)$), hydroxyapatite ($Ca_5(PO_4)_3OH$), and β-tricalcium phosphate ($Ca_3(PO4)_2$) [7]. It is reported that $CaCO_3$ precipitation was observed in bench-scale and pilot-scale denitrification reactors using real groundwater [12,13]. The formation of mineral solids inside the biofilm and at its interface with the membrane can impede H_2 and substrates diffusion within the biofilm and the calcification of fibers turns out to be inflexible and appears to induce fiber breakage [7,13].

In order to control the pH induced by the production of base, two methods were adopted. The first one is adding enough buffer solution to stabilize the pH change. Xia et al. [14] studied the simultaneous reduction of nitrate, sulfate, bromate, hexavalent chromium and para-chloronitrobenzene using a continuously stirred hydrogen-based membrane biofilm reactor. KH_2 PO_4 and Na_2HPO_4 were added into the feed medium in the concentration of 181 mg/L and 379 mg/L respectively as not only the nutrient but also the pH buffer. However phosphate is a control index of water quality which can cause surface-water eutrophication [15] and it is easier to make the calcium ion precipitate in the low concentration. This method is efficient and easy in lab-scale tests, but not feasible in practice. The second method is adding acid at a concentration that neutralizes excessive base production from denitrification. Adham et al. [13] added HCl or sparged CO_2 into the reactor to control the pH in the reactor at a set point using a pH-control loop. It was concluded that CO_2 addition was the preferred method for H_2-based autotrophic processes. Nonetheless, Shahin Ghafari et al. found that continuous sparging of CO_2 made solution to be in the acidic range rapidly and any effort to prevent the pH decline would have been useless, which inhibited the denitrification rate [16].

A novel hydrogen-based membrane biofilm reactor with double bundles was used in this research. One bundle of fibers provides H_2 and the other provides CO_2 in a bubbleless way, which is practical for the inclosed reactor. The CO_2 controls the pH and it is also the inorganic carbon source for microorganisms at the same time. Last but not the least, it allows precise control of the CO_2 delivery rate and minimal loss of CO_2 to the atmosphere, which contributes to the CO_2 fixation also. In order to stabilize the pH in the appropriate range, the stoichiometric relationship of pH change to CO_2 supply should be determined. The Fick's first law at a steady state was used to describe CO_2 permeation through membranes:

$$J_m = \frac{D_m}{z_m}(C_{\text{high}} - C_{\text{low}}) = \frac{D_m}{z_m}\left(\frac{\text{PM}}{H} - C_{\text{low}}\right) \quad (1)$$

The CO_2 permeability in Eq. (1) (D_m) can be determined once the operating conditions (P, C_{low}, z_m) are known and the CO_2 flux (J_m) is measured. The existence forms of CO_2 in water are shown below [17]:

$$CO_2 + H_2O \overset{K_1}{\rightleftarrows} H_2CO_3 \overset{K_2}{\rightleftarrows} H^+ + HCO_3^- \overset{K_3}{\rightleftarrows} 2H^+ + CO_3^{2-} \quad (2)$$

At 25 °C, $K_1 = 2.5 \times 10^{-3}$, $K_2 = 1.74 \times 10^{-4}$, $K_3 = 5.6 \times 10^{-11}$. In fact, $K = K_1 \times K_2 = 4.35 \times 10^{-7}$ is the first dissociation constant of the H_2CO_3 we used frequently. It is indicated that more than 99% CO_2 exists in the form of CO_2 molecule in water, and the physical partition which follows Henry's law is predominant in the diffusion process, so we assume that all CO_2 exist in the form of CO_2 molecule in the CO_2 permeation experiment.

The CO_2 flux (J_m) can be calculated by measuring the CO_2 concentration and the flow rate at the steady state. We then used the permeability to interpret MBfR experimental pH results of bioreduction of nitrate to determine the extent to which CO_2

permeation controlled reactor pH based on the mass balance in the influent and effluent [18]. Our results provide direct guidance to the design and operation of this new type MBfR, which uses CO_2 for pH control and as carbon source. The results are also of value for building up a pH control model.

Before the analysis, the following four assumptions are made:

(1) The reactor is a closed system at a constant pressure equivalent to the atmosphere. The effluent of the reactor was exposed to the atmosphere via an outlet of 0.5 cm diameter tubing. CO_2 exchange between the air and the reactor can be neglected.
(2) Phosphate species are not considered as a buffer due to two factors. First, phosphate added as a nutrient and dosed at the stoichiometric requirement for P uptake in biomass synthesis provides negligible phosphate species in the reactor, compared to carbonate species. Second, the concentration of total phosphorus in most natural groundwater is very low due to its precipitation with calcium [19].
(3) Other natural buffering species (e.g., ammonium) also are neglected, because they are trivial compared to the carbonate species, which account for most of the total alkalinity [19].
(4) $Mg(OH)_2$ also is neglected, because it is super-saturated only at pH values that are too high to be relevant for biological treatment.
(5) Activity coefficients are ignored, since most source water for drinking water treatment has a low salinity. This assumption would need to be removed if denitrification were being carried out with high-salinity water, such as regeneration brine from ion exchange [20].

2. Materials and methods

2.1. Experimental setup

Fig. 1 is schematic of the hydrogen-based membrane biofilm reactors (MBfR) used in this study. The MBfR system included a transparent plastic cylinder, silicone pipelines and peristaltic pumps. Both ends of the cylinder were sealed with the plastic ring and the cap for anaerobic environment. Two bundles of hydrophobic polyvinyl chloride hollow fiber membranes with pore size 0.01 μm (Litree Company, Suzhou, China) were submerged inside the cylinder with their top ends connected to the gas (H_2 or CO_2) pipelines and bottom ends plugged. The outside and inner diameters of the fiber are 0.18 cm and 0.12 cm respectively. The reactor was 24 cm in height and 7 cm in inner diameter. In the CO_2 permeation experiment, the number of total hollow fibers was 150 and they were 21 cm long pressurized with high purity CO_2 (99.999%). In the nitrate removal experiment, the number of one bundle of hollow fibers was 130 and they were 18 cm long pressurized with H_2. The number of the other bundle of hollow fibers is 10 (calculated according to the following CO_2 diffusion coefficient in the PVC membrane @ 25 °C) and they were 13 cm long pressurized with high purity CO_2.

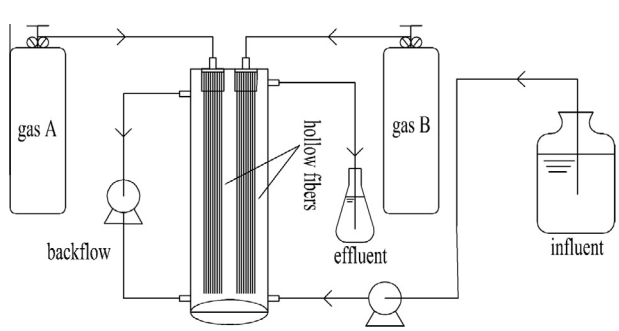

Fig. 1. Schematic of the bench-scale reactor used in the study.

2.2. CO_2 permeation experiment

Fig. 2 is schematic of a bottle with a representative hollow fiber used in the steady state CO_2 permeation experiment. Distilled water free of CO_2 was pumped into the reactor at a flow rate of 2.349×10^{-3} m^3/d. The hollow fibers in the reactor were pressurized with a high purity CO_2 at a pressure of 0.04 MPa. CO_2 diffused through the hollow fiber wall and into the distilled water. A recirculation line provided mixing to ensure that the liquid was completely mixed. The bulk water (100 ml) was sampled regularly and assayed for its CO_2 concentration. Every time we got the sample, we emptied the reactor and started the experiment from the beginning for next sampling time point. Steady state was achieved when the CO_2 concentration was stable.

2.3. Mathematical model to determine the CO_2 permeability

Fig. 3 plots a typical CO_2 concentration profile in the permeation test. The method to measure the permeability of CO_2 through the membrane was adapted from the method to measure the permeability of hydrogen in Youneng Tang [21]. According to Fig. 3, the CO_2 mass balance at steady state in the reactor is

$$QC_i - QC_e = -J_m A_m = -J_l A_l \tag{3}$$

In which

$$J_m = \frac{D_m}{z_m}\left(\frac{PM}{H} - C_l\right) \tag{4}$$

$$J_l = \frac{D_l}{z_l}(C_l - C_e) \tag{5}$$

$$A_m = \pi(d_m - z_m)L_m n_m \tag{6}$$

$$A_l = \pi(d_m + z_l)L_m n_m \tag{7}$$

$$z_l = 2.1 \times 10^{-4} e^{-6.8\times10^{-3}u} \tag{8}$$

$$S = \frac{V}{h} \tag{9}$$

$$u = \frac{Q_t}{S} \tag{10}$$

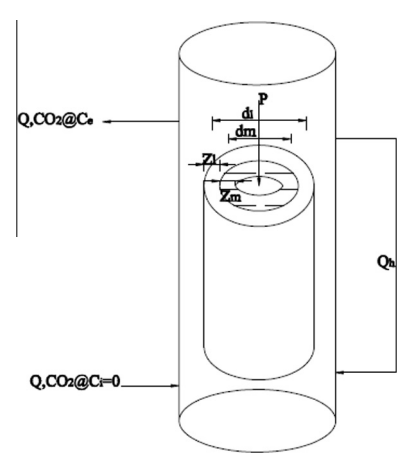

Fig. 2. Schematic diagram of the CO_2 permeation experiment.

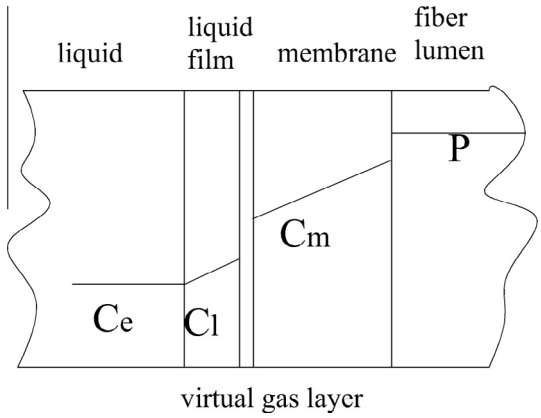

Fig. 3. A typical CO_2-concentration profile in the permeation experiment.

The liquid film thickness (z_l) is determined using an empirical Eq. (8) [22], which is a function that involves the flow shear velocity. We use a representative flow shear velocity (u) that is expressed as the total flow rate (Q_t) through the valid cylinder cross-section (S). Once we measured C_e and substituted Eqs. (4)–(10) into Eq. (3) correspondingly, the only unknown is D_m and C_l in two linearly independent equations. Therefore, we can get D_m.

2.4. Bioreduction of nitrate experiment

The cultivation of autohydrogentrophic organisms was implemented in the physiologic salt water bottle, the same method as in Xia et al. [23]. The composition of the synthetic wastewater was (mg/L): $NaNO_3$ 60.7, $NaHCO_3$ 110, $MgCl_2$ 10, $FeSO_4{\cdot}7H_2O$ 1, $ZnSO_4{\cdot}7H_2O$ 0.013, H_3BO_3 0.038, $CuCl_2{\cdot}2H_2O$ 0.001, $Na_2MoO_4{\cdot}2H_2O$ 0.004, $MnCl_2{\cdot}4H_2O$ 0.004, $CoCl_2{\cdot}6H_2O$ 0.025, $NiCl_2{\cdot}6H_2O$ 0.001, and Na_2SeO_3 0.003. $Na_2HPO_4{\cdot}12H_2O$ 663.3 mg/L and KH_2PO_4 292.3 mg/L were added into the feed water to stabilize the pH throughout the process. The dissolved oxygen in the influent was 8.6 ± 0.2 mg/L. 50 mL cultivation liquid was injected into the reactor by a sterilized syringe. After that, the reactor was fed by 10 mg/L NO_3^- –N with flow of 0.2 mL/min for 24 h. The H_2 supply pressure was set at 0.02 Mpa. An initial biofilm attached to the surface of the membrane fibers was observed. The influent was increased to a flow of 1.0 mL/min and H_2 pressure was increased to 0.04 MPa for biofilm accumulation, which is sufficient for the bioreduction of nitrate [24]. From day 7, the effluent was sampled. Then we began to use KH_2PO_4 (6.5 mg/L) instead of the phosphate buffer pair as the nutrient, and adjust the influent pH to around 7.10. The hollow fiber membranes, inflated with CO_2, were submerged into the reactor. In order to evaluate if the added CO_2 was sufficient or not, we decreased the $NaHCO_3$ dose into the influent water to 40 mg/L and then to 0 mg/L. Effluent NO_3^-, NO_2^-, dissolved oxygen concentration and pH were monitored daily throughout the experiment. All experiments were conducted at ambient temperature (25 ± 1 °C) controlled by the air conditioner.

2.5. Sampling and analysis

All the fluid samples were filtered immediately through a 0.22 μm polyether sulfone syringe filter (Anpel Company, Shanghai, China) and kept in the refrigerator at 4 °C. Nitrate and nitrite were determined by ion chromatograph (ICS-1000, Dionex, USA) using an AS-20 column, an AG-20 precolumn, and a 150-mg/L injection loop [25]. The titration method was used to determine the CO_2 in the bulk water [26]. The pH value and dissolved oxygen concentration were measured with a HQ40d meter (HACH, USA).

3. Results and discussion

3.1. CO_2 permeability and the calculation of membrane area

In the CO_2 permeation experiment, when the system was operated with a high CO_2 pressure (0.06 Mpa) and a low water flow rate (0.72×10^{-3} m^3/d), the water close to the membrane became supersaturated and bubbles were formed on the membrane surface [27]. It changed the surface character and these experimental results were not used. The CO_2 pressures in the lumen of the fibers was set at 0.04 Mpa and the flow rate was 2.349×10^{-3} m^3/d. The recirculation rate was set at 20.655×10^{-3} m^3/d. The concentration of CO_2 in the bulk liquid is plotted in Fig. 4. The concentration of CO_2 in the bulk liquid reached steady state and ended up with the average steady state CO_2 concentration of 149.15 mg/L. Substitute the CO_2 concentration and the experimental parameters in Table 1 into Eqs. (3)–(10), we can get CO_2 D_m value of 3.8375×10^{-7} m^2/d @ 25 °C for the PVC hollow fibers.

According to the D_m calculated above and the CO_2 demand flux determined on the fluxes of oxidized compounds and the stoichiometric coefficient from Eqs. (11)–(12) below, which we obtained from other research [18,21], the area of the membrane can be specified for CO_2 for a specific contaminant loading rate.

$$NO_3^- + 0.23CO_2 + H^+ + 3.03H_2 = 0.48N_2 + 0.046C_5H_7O_2N + 3.37H_2O \tag{11}$$

$$O_2 + 0.028NO_3^- + 0.14CO_2 + 0.028H^+ + 2.39H_2 = 0.028C_5H_7O_2N + 2.31H_2O \tag{12}$$

In the reactor, the CO_2 supplied by the membrane aeration is used in three aspects: the first part is used to neutralize the base produced in the bioreduction of nitrate $\left(44 \times Q_1 \left(\frac{C_{NO_3^-} - \frac{C_{O_2}}{32} \times 62 \times 0.028}{62} \times 1 + \frac{C_{O_2}}{32} \times 0.028\right)\right)$, the second part is used as the carbon source $\left(44 \times Q_1 \left(\frac{C_{NO_3^-} - \frac{C_{O_2}}{32} \times 62 \times 0.028}{62} \times 0.23 + \frac{C_{O_2}}{32} \times 0.14\right)\right)$,

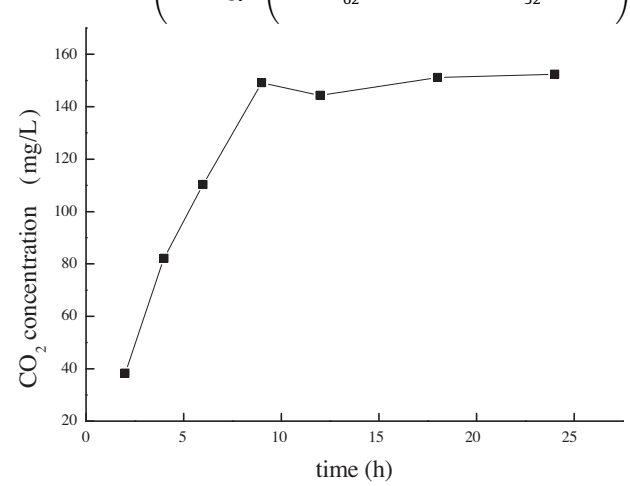

Fig. 4. The concentration of CO_2 in the bulk liquid during the CO_2 permeation experiment.

Table 1
Value of the parameters used in the CO_2 permeation experiment.

Parameter	Value	Units	Parameter	Value	Units
C_e	149.15	g/m^3	P_0	0.04	Mpa
C_i	0	g/m^3	Q	2.349×10^{-3}	m^3/d
d_m	1.8×10^{-3}	m	Q_t	20.655×10^{-3}	m^3/d
h	0.24	m	V	0.814×10^{-3}	m^3
L_{m1}	0.21	m	z_m	0.0003	m
n_m	150				

and the last part forms the HCO_3^-/H_2CO_3 buffer pair to maintain the pH at 7.37, which accounts for one tenth of HCO_3^- $\left(0.1 \times 44 \times Q_1\left(\frac{C_{NO_3^-} - \frac{C_{O_2}}{32} \times 62 \times 0.028}{62} \times 1 + \frac{C_{O_2}}{32} \times 0.028\right)\right)$.

$$J_m A_m = \frac{D_m}{z_m}\left(\frac{PM}{H} - C_l\right)A_m = \frac{D_m}{z_m} \times \frac{PM}{H} \times A_m = 44 \times Q_1\left[\frac{C_{NO_3^-} - \frac{C_{O_2}}{32} \times 62 \times 0.028}{62} \times (1 \times 1.1 + 0.23) + \frac{C_{O_2}}{32} \times (0.028 \times 1.1 + 0.14)\right] = 44 \times Q_1 \times (0.02145C_{NO_3^-} + 0.00417C_{O_2}) \quad (13)$$

We can calculate the number of the fibers according to the concentration of NO_3^- and O_2, the D_m of the membrane, which is calculated before, and the parameter about the fibers in Table 2. The concentration of CO_2 (less than 1 mg/L) in the water to form the HCO_3^-/H_2CO_3 buffer pair is very low compare to the $\frac{PM}{H}$ (1996 mg/L), thus we neglect it to simplify the calculation. That is why we design 10 13 cm long fiber to provide the CO_2 at 0.04 Mpa @ 25 °C. We can find that once the area of the membrane is fixed, we can only adjust the CO_2 flux in a small range by the pressure under 0.08 Mpa considering that air bubbles are formed at pressures larger than 0.08 Mpa. In fact, the original reactor was set up with two identical bundles of hollow fibers for CO_2 and H_2 separately. Each bundle contains 130 18 cm hollow fibers. The pH of the effluent decreased rapidly to below 5 even when the CO_2 pressure was set at 0.01 Mpa, the least count of the valve. In order to keep the pH in the appropriate range, it is important to determine the area of the membrane providing the CO_2. Certainly, the actual micropolluted raw water is more complex, and we should take all the oxidized compound into consideration. The following is the oxidized compound which may exist in the micropolluted water and participate in reaction [18,21]:

$$SO_4^{2-} + 0.015NO_3^- + 0.075CO_2 + 1.52H^+ + 4.21H_2 = 0.5H_2S + 0.5HS^- + 0.015C_5H_7O_2N + 4.17H_2O \quad (14)$$

$$ClO_4^- + 0.11NO_3^- + 0.53CO_2 + 0.11H^+ + 5.48H_2 = Cl^- + 0.11C_5H_7O_2N + 5.15H_2O \quad (15)$$

$$SeO_4^{2-} + 0.027NO_3^- + 0.13CO_2 + 2.03H^+ + 3.38H_2 = Se + 0.027C_5H_7O_2N + 4.3H_2O \quad (16)$$

Table 2
Value of the parameter about the CO_2 fiber in nitrate bioreduction experiment.

Parameter	Value	Units
$C_{NO_3^-}$	10	g/m^3
C_{O_2}	8.7	g/m^3
L_{m2}	0.13	m
Q_1	1.44×10^{-3}	m^3/d

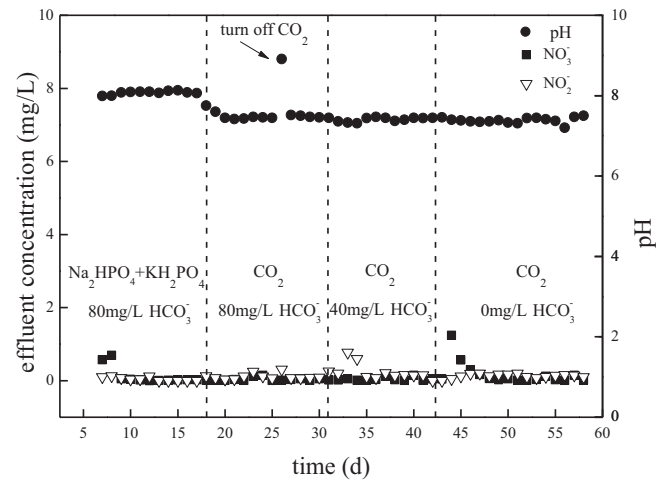

Fig. 5. The effluent concentration of NO_3^- NO_2^- and pH in the different phase of nitrate bioreduction experiment.

3.2. Nitrate bioreduction and effect of sodium bicarbonate

Fig. 5 presents the experimental results for the startup and steady-state of the bioreduction of nitrate experiment. The dissolved oxygen in the effluent was 0.3 ± 0.1 mg/L in the process, which is consistent with other research [5,28,29] NO_3^-–N decreased to 0.6 mg/L on day 7 and below 0.05 mg/L on day 9 stepwise. Meanwhile, effluent NO_2^-–N was 0.1 mg/L and decreased to 0 on day 13 stepwise. NO_2^-–N accumulation was not detected in the effluent. The pH was in the range of 7.99–8.13 during this period. The reactor was run in this condition for 11 days, and the total nitrogen removal rate reached above 99.7%. The biofilm was considered as mature and ready for subsequent operation with the appearance of a tan film attached to the surface of the membrane fibers. On day 18, the CO_2 was introduced into the reactor instead of phosphate buffer pair in high concentration. On day 20, the phosphate in the effluent was very low and stable, which suggested that the phosphate buffer pair had been washed out and the pH decreased to 7.45 gradually. From day 18 to day 31, the nitrate was reduced completely throughout the process. On day 25, the flow valve of CO_2 was shut off, and the pH increased to 8.91 on day 26 acutely. We turned on the valve of CO_2 immediately. On day 27, the pH decreased to 7.52 and was stable in the range of 7.5–7.45 in the following 3 days. This means that the CO_2 is efficient to control the pH in the reactor and keep the reactor run stable in the appropriate pH range. The CO_2 flux based on the measured CO_2 diffusion coefficient would satisfy the stoichiometry for the denitrification of NO_3^-. Thus, the influent concentration of HCO_3^- of 80, 40, 0 mg/L was investigated to find whether CO_2 provided by the membrane aeration was sufficient for the autotrophic denitrifiers. On day 32, the influent HCO_3^- concentration was decreased to 40 mg/L, and the total nitrogen removal rate decreased to 91.8% and recovered to >97% on day 36 quickly. The pH was stable at around 7.40. On day 42, influent HCO_3^- concentration was further decreased to 0. From day 43 to day 44, the total nitrogen removal rate decreased from 99% to 87% in one day and then the total nitrogen removal rate increased above 95% stepwise, which means that the CO_2 was adequate to keep the reactor robust. When the inorganic carbon source concentration satisfies the demand of the microorganism, higher dose of bicarbonate does not necessarily result in better removal, which agrees with other researchers [30]. In fact, the inorganic carbon source is sufficient in the groundwater [31–33], which may not be a problem in treating polluted groundwater.

4. Conclusion

Considering the air tightness of the membrane module, the pressure of the gas should be below 0.08 Mpa to make the module safe to operate. Therefore, to adjust the CO_2 flux through the pressure change is limited to a small range, once the area of the membrane is fixed. So it is important to get the diffusion coefficient (D_m) to design a rational area of membrane according to the base produced by the oxidized contaminants in the influent water to control the pH in the reactor in optimal range. The Fick's first law and steady state experiment were precise and simple to be adopted to solve the D_m of the polyvinyl chloride membrane used in this study, which is 3.8375×10^{-7} m^2/d @ 25 °C.

According to the D_m solved in the CO_2 permeation experiment and the fluxes of oxidized compounds, we design a membrane biofilm reactor with double bundles of fiber, one for H_2 supply and the other for CO_2 supply. The CO_2 can stabilize the pH in the reactor at appropriate value of 7.4 approximately with more than 99% total nitrogen removed. This novel membranes biofilm reactor was stable and efficient in nitrate removal.

Acknowledgment

This work was financially supported by the National Natural Science Foundation of China (No. 51378368).

References

[1] B.E. Rittmann, The membrane biofilm reactor is a versatile platform for water and wastewater treatment, Environ. Eng. Res. 12 (2007) 157–175.
[2] B.E. Rittmann, The membrane biofilm reactor: the natural partnership of membranes and biofilm, Water Sci. Technol. 53 (2006) 219–225.
[3] B. Rittmann, R. Nerenberg, K. Lee, I. Najm, T. Gillogly, G. Lehman, S. Adham, Hydrogen-based hollow-fiber membrane biofilm reactor (MBfR) for removing oxidized contaminants, Water Supply 4 (2004) 127–133.
[4] S.Q. Xia, F.H. Zhong, Y.H. Zhang, H.X. Li, X. Yang, Bio-reduction of nitrate from groundwater using a hydrogen-based membrane biofilm reactor, J. Environ. Sci.-China 22 (2010) 257–262.
[5] R. Nerenberg, B.E. Rittmann, Hydrogen-based, hollow-fiber membrane biofilm reactor for reduction of perchlorate and other oxidized contaminants, Water Sci. Technol. 49 (2004) 223–230.
[6] A.I. Alabdula'aly, A.M. Al-Rehaili, A.I. Al-Zarah, M.A. Khan, Assessment of nitrate concentration in groundwater in Saudi Arabia, Environ. Monit. Assess. 161 (2010) 1–9.
[7] K.-C. Lee, B.E. Rittmann, Effects of pH and precipitation on autohydrogenotrophic denitrification using the hollow-fiber membrane-biofilm reactor, Water Res. 37 (2003) 1551–1556.
[8] Y.N. Tang, C. Zhou, M. Ziv-El, B.E. Rittmann, A pH-control model for heterotrophic and hydrogen-based autotrophic denitrification, Water Res. 45 (2011) 232–240.
[9] J. Baeseman, R. Smith, J. Silverstein, Denitrification potential in stream sediments impacted by acid mine drainage: effects of pH, various electron donors, and iron, Microb. Ecol. 51 (2006) 232–241.
[10] V. Janda, J. Rudovský, J. Wanner, K. Marha, In situ denitrification of drinking water, Water Sci. Technol. 20 (1988) 215–219.
[11] M. Kurt, I. Dunn, J. Bourne, Biological denitrification of drinking water using autotrophic organisms with H_2 in a fluidized-bed biofilm reactor, Biotechnol. Bioeng. 29 (1987) 493–501.
[12] M.C. Ziv-El, B.E. Rittmann, Systematic evaluation of nitrate and perchlorate bioreduction kinetics in groundwater using a hydrogen-based membrane biofilm reactor, Water Res. 43 (2009) 173–181.
[13] S. Adham, E.V.W. District, Membrane Biofilm Reactor Process for Nitrate and Perchlorate Removal, AWWA Research Foundation, 2004.
[14] S. Xia, J. Liang, X. Xu, S. Shen, Simultaneous removal of selected oxidized contaminants in groundwater using a continuously stirred hydrogen-based membrane biofilm reactor, J. Environ. Sci. 25 (2013) 96–104.
[15] D.L. Correll, The role of phosphorus in the eutrophication of receiving waters: a review, J. Environ. Qual. 27 (1998) 261–266.
[16] S. Ghafari, M. Hasan, M.K. Aroua, Effect of carbon dioxide and bicarbonate as inorganic carbon sources on growth and adaptation of autohydrogenotrophic denitrifying bacteria, J. Hazard. Mater. 162 (2009) 1507–1513.
[17] W. Lianbo, Z. Yulin, The Foundation of Modern Chemistry Chemical Industry Press, 1987 (in Chinese).
[18] E.R. Bruce, L.M. Perry, Environmental Biotechnology: Principles and Applications, McGrawHill, New York, 2001. 400.
[19] V. Snoeyink, D. Jenkins, Water Chemistry, John Wiley & Sons Inc., New York, 1980.
[20] S.W. Van Ginkel, C.H. Ahn, M. Badruzzaman, D.J. Roberts, S.G. Lehman, S.S. Adham, B.E. Rittmann, Kinetics of nitrate and perchlorate reduction in ion-exchange brine using the membrane biofilm reactor (MBfR), Water Res. 42 (2008) 4197–4205.
[21] Y. Tang, C. Zhou, S.W. Van Ginkel, A. Ontiveros-Valencia, J. Shin, B.E. Rittmann, Hydrogen permeability of the hollow fibers used in H_2-based membrane biofilm reactors, J. Membr. Sci. 407 (2012) 176–183.
[22] G.H. Chen, J.C. Huang, Determination of diffusion layer thickness on a biofilm, J. Environ. Sci. Health Part A 31 (1996) 367–386.
[23] S. Xia, S. Shen, J. Liang, X. Xu, Study on removing selenate from groundwater by autohydrogenotrophic microorganisms, Front. Environ. Sci. Eng. (2013) 1–7.
[24] S.Q. Xia, Y.H. Zhang, F.H. Zhong, A continuous stirred hydrogen-based polyvinyl chloride membrane biofilm reactor for the treatment of nitrate contaminated drinking water, Bioresour. Technol. 100 (2009) 6223–6228.
[25] S.Q. Xia, Z.Q. Zhang, F.H. Zhong, J.A. Zhang, High efficiency removal of 2-chlorophenol from drinking water by a hydrogen-based polyvinyl chloride membrane biofilm reactor, J. Hazard. Mater. 186 (2011) 1367–1373.
[26] S.E.P. Administration, Monitoring and Analysis Methods for Water and Wastewater, 4th ed., Beijing, China, 2002.
[27] T. Ahmed, M.J. Semmens, M.A. Voss, Oxygen transfer characteristics of hollow-fiber, composite membranes, Adv. Environ. Res. 8 (2004) 637–646.
[28] H.P. Zhao, Z.E. Ilhan, A. Ontiveros-Valencia, Y.N. Tang, B.E. Rittmann, R. Krajmalnik-Brown, Effects of multiple electron acceptors on microbial interactions in a hydrogen-based biofilm, Environ. Sci. Technol. 47 (2013) 7396–7403.
[29] S.W. Van Ginkel, C. Zhou, M. Lien, B.E. Rittmann, Hydrogen-based nitrate and selenate bioreductions in flue-gas desulfurization brine, J. Environ. Eng.-ASCE 137 (2011) 63–68.
[30] S. Ghafari, M. Hasan, M.K. Aroua, Improvement of autohydrogenotrophic nitrite reduction rate through optimization of pH and sodium bicarbonate dose in batch experiments, J. Biosci. Bioeng. 107 (2009) 275–280.
[31] M. Arunprakash, L. Giridharan, R. Krishnamurthy, M. Jayaprakash, Impact of urbanization in groundwater of south Chennai City, Tamil Nadu, India, Environ. Earth Sci. 71 (2014) 947–957.
[32] R.W. Healy, T.T. Bartos, C.A. Rice, M.P. McKinley, B.D. Smith, Groundwater chemistry near an impoundment for produced water, Powder River Basin, Wyoming, USA, J. Hydrol. 403 (2011) 37–48.
[33] G. Zhu, Z. Li, Y. Su, J. Ma, Y. Zhang, Hydrogeochemical and isotope evidence of groundwater evolution and recharge in Minqin Basin, Northwest China, J. Hydrol. 333 (2007) 239–251.
[34] J.W. Mutoru, A. Leahy-Dios, A. Firoozabadi, Modeling infinite dilution and Fickian diffusion coefficients of carbon dioxide in water, Aiche J. 57 (2011) 1617–1627.
[35] G.F. Versteeg, W. Van Swaalj, Solubility and diffusivity of acid gases (carbon dioxide, nitrous oxide) in aqueous alkanolamine solutions, J. Chem. Eng. Data 33 (1988) 29–34.